Transformation of iridium(110) (1×1) into (1×2) and spatial distribution of reactive carbon dioxide desorption

Tatsuo Matsushima, Yuichi Ohno, and Kiyoshi Nagai
Institute for Molecular Science, Myodaiji, Okazaki 444, Japan

(Received 6 September 1990; accepted 24 September 1990)

The spatial distribution of the desorption flux of CO_2 produced on Ir(110) (1×1) and (1×2) surfaces was studied by means of angle-resolved thermal desorption and low-energy electron diffraction. The distribution is collimated along the bulk surface normal on (1×1). It is sharp in the [001] direction and sharper in the [1$\bar{1}$0] direction. This distribution is consistent with the model that the reactive desorption occurs on a short bridge site. On (1×2) surfaces, two-directional desorption was observed, which was collimated along the axis at the polar angle of 26 deg in both [001] and [00$\bar{1}$] directions. The distribution in the [1$\bar{1}$0] direction is collimated along the bulk surface normal. The reactive desorption was suggested to take place on a threefold hollow site on the declining terrace. The spatial distribution changed from the (1×1) type to the (1×2) type during the transformation of the surface structure. This structure change was confirmed by low-energy electron diffraction.

I. INTRODUCTION

Dynamic properties of chemical processes on solids depend on surface structure, especially the structure of the reaction sites. To design new functional surfaces, this structure should be analyzed. So far the structure has been speculated from structural information of nonreacting surface species, which can be obtained by several methods, such as vibrational spectroscopies and diffraction methods. The structure must be more directly analyzed through the reaction itself. However, no structural information has been provided by classical chemical kinetics, which treats the elementary reaction rate as a function of reactant coverages.

We have previously shown the possibility of reaction dynamics sensitive to the structure of the reaction site.[1,2] In some combinative desorptions the spatial distribution of the product desorption provides structural information on the reaction site.[3,4] The product is likely to be repulsed by the surface during formation,[5] and the shape of the repulsive potential is preserved in the spatial and velocity distributions.

In this paper we will report on the spatial distribution of reactive CO_2 desorption during the transformation of Ir(110)(1×1) into (1×2). This is the first observation on the variation of the spatial distribution during the structural changing of the reaction site.

We reported previously that the orientation of the reaction site was preserved in the spatial distribution of the desorption flux of CO_2 produced on Pt(110)(1×2) and Ir(110)(1×2) reconstructed surfaces.[4,6] Both surfaces are explained by the missing-row model, where every second row in the [1$\bar{1}$0] direction is missing.[7–12] The surface consists of three-atom-wide terraces of a (111) structure declining at about 30 deg in either the [001] or [00$\bar{1}$] direction.[8] Two-directional desorption of produced CO_2 was observed at the desorption angle of 21–26 deg, concluding that the CO oxidation took place on the declining terrace.[4,6] On the other hand, the desorption of CO_2 produced on Pt(110)(1×1) was estimated to be collimated along the bulk surface normal.[4(b)]

The metastable structure of Pt(110)(1×1) is easily transformed into (1×2) by being heated above 300 K without adsorbed CO.[13,14] It is difficult to keep this structure with small amounts of adsorbed CO at higher temperatures. This indicates the difficulty in the usage of the angle-resolved thermal desorption for measurements of the spatial distribution on this surface.[4] On the other hand, the unreconstructed structure of Ir(110)(1×1) can be stabilized by oxygen,[15] and the transformation into (1×2) is slow.[9–11] Thus we have succeeded in observing the variation in the spatial distribution of reactive CO_2 desorption during this transformation.

II. EXPERIMENTAL

The experimental procedures were essentially the same as those reported previously.[16] The apparatus consisted of a reaction chamber with low-energy electron diffraction (LEED)-Auger electron spectroscopy (AES), a collimator, and an analyzer chamber. The flux of CO_2 molecules desorbing from the surface and passing through the collimator slits contributed mostly to the signal of the mass spectrometer in the analyzer chamber (angle-resolved spectra). The CO_2 formation was also recorded with another mass spectrometer in the reaction chamber (angle-integrated spectra).

An iridium crystal with (110) faces was set on a sample holder, which allowed the rotation of the crystal azimuth ϕ and also of the desorption angle (the polar angle) θ. The (1×2) structure was prepared by heating (at 1450 K for about 10 min) a clean surface judged by AES and with no CO formation during heating after oxygen exposure. The diffraction spot at the half-order positions appeared somewhat streaked in the [001] direction. This surface is referred to as (1×2) in the present experiments.

The (1×1) surface was prepared in the manner reported by Chan *et al.*[15] The crystal was heated in 5×10^{-8} Torr of O_2 for five min at 850 K and cooled to room temperature. At this stage, the surface showed a $c(2\times2)$-O lattice. No LEED spots were visible at ($\pm$ 1, $\pm$ 1/2). Excess chemis-

 0021-9606/91/010704-07$03.00

orbed oxygen was removed by a few cycles of CO exposure at 200 K and heating to 570 K. The resultant surface showed a (1×1) structure without any superstructure spots. This surface was used as (1×1). This temperature of 570 K was necessary to remove most of $CO(a)$, however, the transformation into (1×2) might somewhat proceed. This surface is still covered by oxygen probably in the oxide form or absorbed beneath the surface, since this oxygen is nonreactive toward CO or hydrogen.

The surface was exposed to $^{18}O_2$ at 270 K and then to $C^{16}O$ around 200 K. It was heated at a rate of 10 K/s, while the desorption of the product $C^{16}O^{18}O$ was monitored in both angle-resolved and angle-integrated forms. In the following, oxygen 18 will sometimes be denoted simply as O, since the product consists merely of $C^{16}O^{18}O$.

III. RESULTS

A. Transformation of (1×1) into (1×2)

The (1×1) surface prepared above was transformed into the (1×2) form by heating above 570 K. The intensity of the half-order LEED spot at (1, 1/2) was monitored at an accelerating voltage of $E_0 = 48$ eV with a spot photometer during sequential heating from 300 up to 1450 K. The sample was heated at a rate of 10 K/s and cooled immediately after a desired temperature T_P was reached. The photointensity in the dotted circle shown in the insert in Fig. 1 was measured at 200 K. The results are shown as curve (a) in the figure. The intensity remained invariant below $T_P = 500$ K and decreased sharply above it. This decrease was due to the removal of CO adsorbed during preparation of the (1×1) structure. The intensity showed a minimum around $T_P = 550$ K and increased sharply above it. No background intensity was subtracted in the present experiments. The intensity increased sharply in the range of 550 to 800 K, indicating that the transformation into (1×2) took place in this temperature range. However, it did not necessarily mean that the transformation into (1×2) was completed around 800 K. The spot was still streaked along the [001] direction and the spot photometer accepted the signal from a round area centered at (1, 1/2). In fact, the transformation continued at higher temperatures as described in Sec. III F. On the other hand, the intensity of the integral order spot at (1,0) with $E_0 = 46$ eV decreased by only about 15% in the range of 550–800 K.

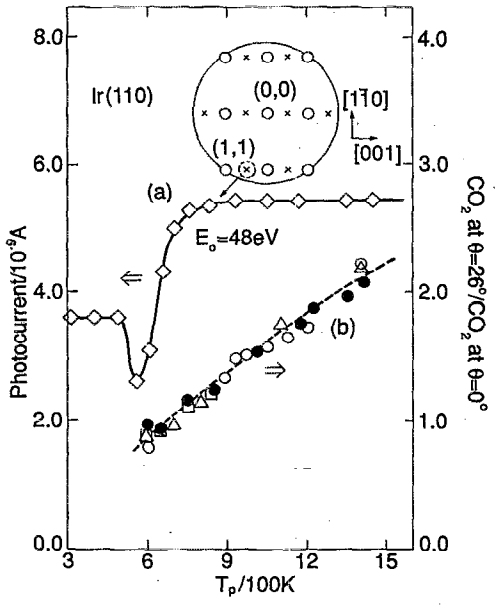

FIG. 1. Transformation of the (1×1) structure into the (1×2) form. (a) The intensity of a half-order spot in LEED was monitored as a function of heating temperature T_P. A typical LEED pattern is shown in the insert. The open circles indicate integral order spots and the crosses half-order spots. (b) The ratio of the CO_2 peak height at $\theta = 26°$ in the [001] direction to that at $\theta = 0°$. CO_2 was generated at $\theta_0/\theta_{0.MAX} = 0.6$ and 0.6 L CO. Results in four series are summarized.

B. Adsorption of CO and O

Oxygen and CO adsorb quickly below room temperature. The coverages were determined by thermal desorption. Oxygen desorbed above 700 K. The peak area reached a steady value above 6 L (1 Langmuir $= 1\times10^{-6}$ Torr s) on both (1×1) and (1×2) surfaces. The coverage was normalized to the value at saturation and represented as $\theta_0/\theta_{0.MAX}$. On the other hand, the desorption of CO was observed above 500 K after small exposures. It was extended to low temperatures with increasing exposure. The desorption area increased linearly below 1 L. It reached a steady value above 10 L.

The coadlayer was prepared by oxygen adsorption at 270 K followed by CO exposure at 200 K. The adsorption of CO was not retarded by preadsorbed oxygen at small CO coverages. However, the saturation level of CO was suppressed strongly by preadsorbed oxygen. For example, only about half of the oxygen was removed as CO_2 when a large CO exposure was applied at $\theta_0/\theta_{0.MAX} = 0.60$, although no excess CO was desorbed. The structure of the coadlayer was not analyzed this time, since fractional order spots in the LEED screen were obscured by the sample holder.

C. CO_2 formation spectra

Typical CO_2 formation spectra observed on (1×1) are summarized in Fig. 2(a). The surface precovered by oxygen 18 at various coverages was exposed to 0.6 L CO at 200 K. At small oxygen coverages, a single peak, P_1-CO_2, was observed around 550 K. With increasing oxygen coverage, another peak, P_2-CO_2, appeared around 380 K. This peak shifted somewhat to lower temperatures at high oxygen coverages, where the other peak was largely attenuated.

Tracer experiments indicated nonreactivity of oxygen stabilizing the (1×1) structure toward CO. We have examined the isotope composition of CO_2 produced when the (1×1) surface stabilized by oxygen 18 was exposed to $^{16}O_2$ and then $C^{16}O$. Only $C^{16}O_2$ was produced and no $C^{16}O^{18}O$ was observed. Oxygen involving ^{18}O predosed was desorbed above 1000 K, although the desorption of $^{16}O_2$ started around 700 K. This means no participation of oxygen 18 predosed in the CO oxidation.

The right panel summarizes CO_2 spectra observed simultaneously in the angle-resolved form at the surface normal. P_2-CO_2 was enhanced as compared with P_1-CO_2, indi-

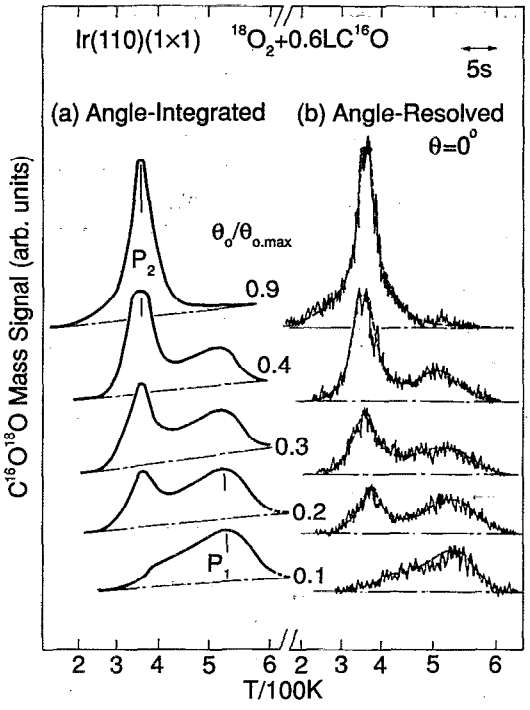

FIG. 2. Typical CO_2 formation spectra generated at various oxygen coverages in both (a) angle-integrated and (b) angle-resolved form. The (1×1) surface was exposed to $^{18}O_2$ at 270 K and further to 0.6 L CO at 200 K, and finally heated at a rate of 10 K/s to 570 K to proceed the reaction. The dashed curves indicate the signal after smoothing procedures.

cating that the desorption of the former was more sharply collimated along the surface normal.

CO_2 spectra generated on (1×2) were quite similar to those on (1×1) except for the small P_1-CO_2 formation peak. This peak was noticeable at small oxygen coverages and disappeared at high θ_0. These results are consistent with earlier work by Weinberg's group, where P_1-CO_2 was due to the reaction on oxide-covered surfaces.[17]

D. Spatial distribution on (1×1)

The desorption of both P_1- and P_2-CO_2 is sharply collimated along the surface normal. However, the determination of the angular distribution of P_1-CO_2 desorption was not successful because of relatively large noises in the angle-resolved signal. The P_2-CO_2 desorption showed anisotropy in the spatial distribution, depending on the crystal azimuth. The distribution along the surface trough (in the $[1\bar{1}0]$ direction $\phi = 90°$) is shown in Fig. 3. It varied as $(\cos\theta)^{10\pm2}$. The distribution perpendicular to the surface trough ($\phi = 0°$) is also collimated along the surface normal as shown in Fig. 4. It showed $(\cos\theta)^{4\pm1}$ dependence. This is broader than that in the $[1\bar{1}0]$ direction.

The angular distribution varies smoothly between [001] and $[1\bar{1}0]$ direction. The crystal azimuth dependence of the CO_2 signal at a fixed desorption angle is shown in Fig. 5. It shows a maximum in the [001] and a minimum in the $[1\bar{1}0]$ direction, as expected from the angular distributions.

E. Spatial distribution on (1×2)

The distribution of the P_2-CO_2 desorption from (1×2) surfaces is quite different from that on (1×1). The angular distribution is characteristic of two-directional desorption. It is collimated along the axis at $\theta = 26°$ in both [001] and $[00\bar{1}]$ directions. Two series of experiments are summarized in Fig. 6. In series (a), the crystal was heated at 1450 K for 2

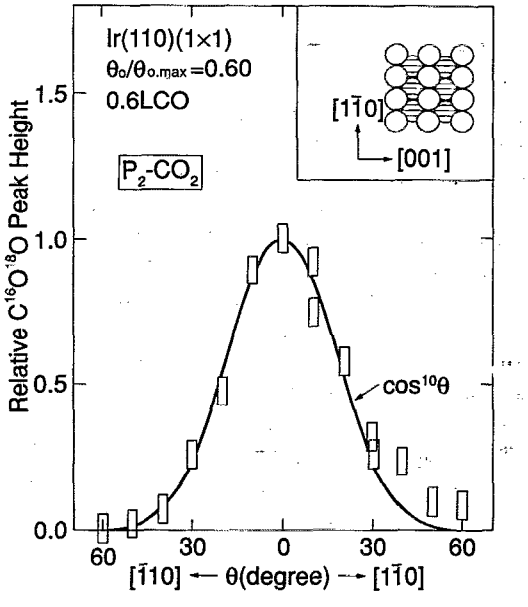

FIG. 3. Angular distribution of the desorption flux of P_2 – CO_2 on (1×1) surfaces in the $[1\bar{1}0]$ direction. A top view of the surface is shown in the insert. The experimental conditions are given in Fig. 2.

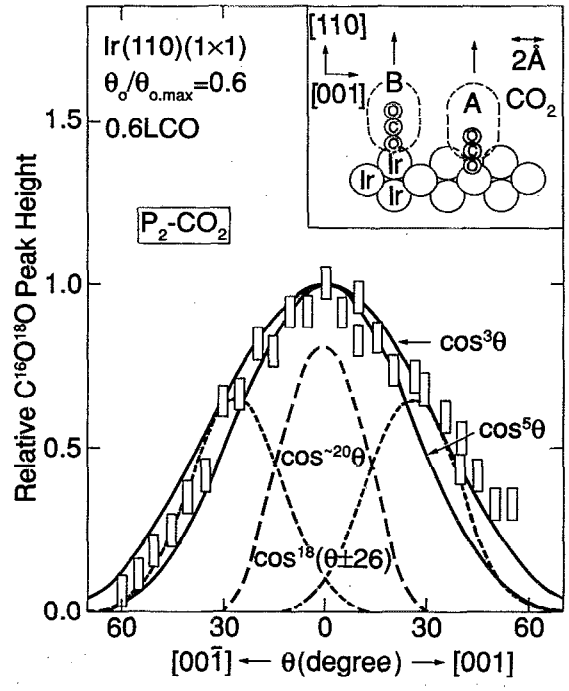

FIG. 4. Angular distribution of P_2 – CO_2 desorption on (1×1) surfaces in the [001] direction. The dotted and dashed curves are explained in the text. A side view of two reaction sites, (A) a long bridge site and (B) a short bridge site, are shown in the insert. The dashed ellipse indicates the size of CO_2 being produced.

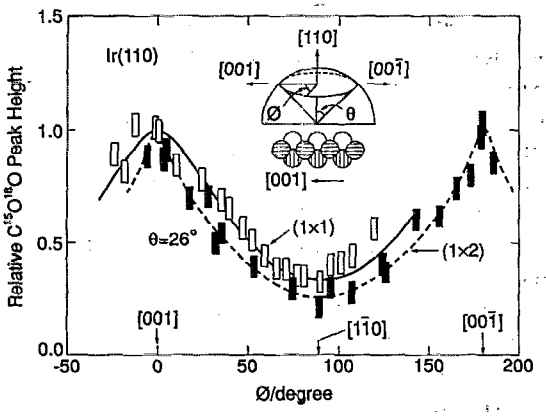

FIG. 5. Crystal azimuth dependence of the P_2 — CO_2 peak height at a fixed desorption angle on (1×1) and (1×2). CO_2 was generated at $\theta_0/\theta_{0.MAX} = 0.6$ and 0.6 L CO. The signal was normalized to the value at $\theta = 26°$ in the [001] direction. It should be noted that the absolute signal at $\theta = 26°$ on (1×1) was much less than the other. The crystal azimuth is defined in the inserted figure.

min before each thermal desorption procedure. In series (b), on the other hand, it was once treated at high temperatures in the same way as above and heated repeatedly up to only 570 K for the CO_2 formation and also for the removal of adspecies from background gasses. The angular distribution was well reproduced in both series, indicating that the transformation of the surface structure was quenched as it was at the heat treatment at 1450 K. This is quite different from the results on Pt(110) (1×2).[4]

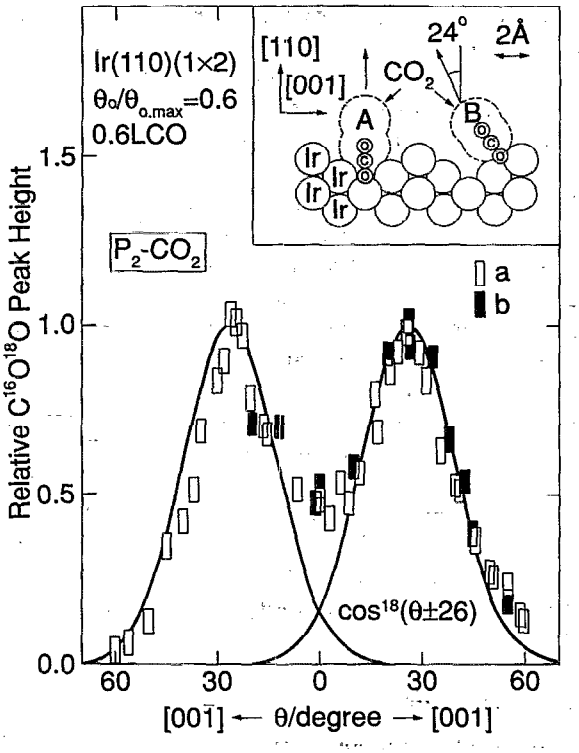

FIG. 6. Angular distribution of the P_2 — CO_2 desorption flux in the [001] direction on (1×2) surfaces. The differences in two series, (a) and (b), are given in the text. The insert shows a side view of the reconstructed surface and also the reaction site on (A) a long bridge site in the trough and (B) a threefold hollow site on the terrace.

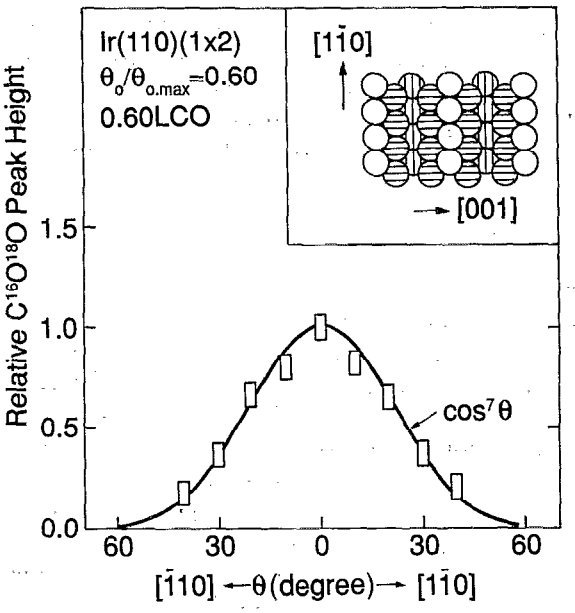

FIG. 7. Angular distribution of the desorption flux of P_2 — CO_2 produced on (1×2) in the [1$\bar{1}$0] direction. A top view of the reconstructed surface is shown in the insert.

Each desorption component shows a very sharp distribution as $(\cos\theta \pm 26)^{18\pm2}$. This CO_2 desorption is collimated only in either the [001] or [00$\bar{1}$] direction. The crystal azimuth dependence of the CO_2 signal is shown in Fig. 5, where all signals were normalized to the value in the [001] direction. The dependence showed maxima in the [001] and [00$\bar{1}$] directions and a minimum in the [1$\bar{1}$0] direction in a similar manner to that on (1×1). However, it should be noted here that the spatial distribution on (1×2) is quite different from that on (1×1). The signals at $\theta = 26°$ on (1×1) were much less than those on (1×2).

The angular distribution in the [1$\bar{1}$0] direction is shown in Fig. 7. It is collimated along the bulk surface normal. It is slightly broader than that in the same direction on (1×1). It varied as $(\cos\theta)^{7\pm1}$.

F. Structure transformation and spatial distribution

In the preceding sections, the spatial distribution of reactive CO_2 desorption was shown to be sensitive to surface structure. It is interesting to examine the variation of the spatial distribution during the transformation of the surface structure. The transformation from (1×1) into (1×2) was controlled by the temperature used for pretreatment.

We have examined the spatial distribution after heating (1×1) surfaces *in vacuo* up to a desired temperature T_P. The crystal was heated at a rate of 10 K/s and was cooled immediately after T_P was reached. The angular distribution was measured in the [001] direction without heating above 570 K after T_P treatment. The distribution changed from the (1×1) type to the (1×2) type with increasing T_P. Here, we represent the change in the spatial distribution by using a compositional ratio, $(CO_2)_{26°\text{ in }[001]}/(CO_2)_{0°}$, where $(CO_2)_{26°\text{ in }[001]}$ is the peak height of the CO_2 signal at $\theta = 26°$ in the [001] direction, and $(CO_2)_{0°}$ at $\theta = 0°$ (the surface normal). The surface is considered to consist of a

mixture of (1×1) and (1×2) patches during the transformation. The above parameter represents the contribution from both patches. The values determined are shown as curve (b) in Fig. 1. Results in four series are summarized. The parameter increased from 0.8 at $T_P = 570$ K to 2.2 at $T_P = 1450$ K with increasing T_P.

IV. DISCUSSION

A. Reaction site

The CO_2 formation proceeds between $CO(a)$ and $O(a)$. This process is part of the reaction pathway of the CO oxidation during the catalyzed reaction at steady state.[18] The reaction site is likely to be on each oxygen adsorption site, since the binding energy of CO to the surface (about 35 kcal/mol[17]) is much less than that of oxygen adatoms (about 90 kcal/mol[20]), and $CO(a)$ is much more mobile than $O(a)$.[19,20] The product molecule is repulsed by the surface immediately prior to the desorption as discussed below, and the shape of the repulsive potential is preserved in the spatial distribution. In the present case, the symmetry and the orientation of the oxygen adsorption site are expected to be preserved in the distribution of the CO_2 desorption.

There are three possible adsorption sites for oxygen: a threefold hollow site on the (111) terrace (TH), a short bridge site on the uppermost atom row (SB), and a long bridge site in the trough (LB). The first is the adsorption site on Ir(111) bulk surfaces.[21] The second has been proposed as the site on Ir(110) (1×1) stabilized by a quarter monolayer of oxygen.[22] The third has been frequently proposed on unreconstructed fcc (110) planes such as Cu(110),[23] Ag(110),[24,25] and Pd(110).[26]

On (1×2) surfaces, two-directional desorption was observed. The components are directed toward the terrace surface normal. It may be concluded that the reactive desorption on (1×2) surfaces takes place on LB sites on the declining terrace, labled B in the insert of Fig. 6. These results, however, do not necessarily mean that on (1×2) surfaces oxygen adsorbs only on the terrace. Oxygen on the terrace is likely to be more reactive toward CO than on the other sites. It has been proposed that CO is adsorbed on the top site in the atom row on (1×2) reconstructed surfaces[14] and may therefore react more easily with oxygen on the terrace rather than in the trough.

On (1×1) surfaces, on the other hand, a single sharp peak, which was collimated along the bulk surface normal, was observed in the angular distribution curve of the CO_2 desorption in both [001] and $[1\bar{1}0]$ directions. The distribution in the $[1\bar{1}0]$ direction is sharper than that in [001]. This disagrees with our previous results on Pd(110)(1×1), where the reaction takes place on LB sites in the trough.[3] The unit cell of the surface including this reaction site is long along the trough and is closely surrounded in the [001] direction by metal atoms in the first layer, as shown in the insert of Fig. 4. The surface parallel mobility of CO_2 being produced is less restricted along the trough, since the space is open in this direction. This situation has been considered to cause a broader angular distribution in the $[1\bar{1}0]$ direction on Pd(110), as compared with that in the [001] direction. In contrast, the present experiments on (1×1) show a broader distribution in the [001] direction.

We considered two possibilities; the first is due to the reactive desorption on SB sites. The other is the possibility that the present (1×1) surface still involves small patches of (1×2) structures undetectable by LEED. In fact, recent medium energy ion scattering experiments have indicated that the (1×1) surface prepared in Chan's manner still contains about 15% of (1×2) patches,[12] although this value has not been accurately determined. Therefore, we deconvoluted the angular distribution curve in the [001] direction. The results are shown by the dotted and dashed curves in Fig. 4. In these procedures, the contribution of the two-directional desorption of the $(\cos\theta \pm 26)$[18] form was first fitted with the data above $\theta = 26°$. The contribution from (1×1) was derived as the difference between the observed signals averaged as $(\cos\theta)^4$ and the tow-directional desorption components. The resultant component as shown by the dashed curve is collimated along the bulk surface normal as $(\cos\theta)^{\sim 20}$. This distribution is sharper than that in the $[1\bar{1}0]$ direction. The resultant spatial distribution on (1×1) agrees well with the model that the reactive desorption occurs on LB sites.[3] However, the contribution from (1×2) patches estimated in Fig. 4 was about two-thirds of the total formation, much more than 15%. This is unreasonable, although the fraction of CO_2 formation on both surfaces is not necessarily expected to be equal to the surface composition.

The reactive desorption on SB sites is more plausible. The unit cell of the surface lattice involving this reaction site is long in the [001] direction and short along the trough.[3] Furthermore, there is a large free space around the site in both [001] and $[00\bar{1}]$ directions. Therefore, it is expected that the angular distribution of CO_2 desorption is collimated along the bulk surface normal, and that the distribution perpendicular to the surface trough is broader than that along it. This is in good agreement with the experimental results.

The spatial distribution may be insufficient to assign the reaction site. The velocity distribution analysis of desorbing CO_2 should be more sensitive to the structure of the site. It will differentiate the above cases more clearly. The mean velocity of desorbing CO_2 produced shows the highest value in the direction where the desorption flux is maximized.[5,27,28] Therefore, in the former case, the velocity at 26° in the [001] direction is expected to be high because the CO_2 at this position would be mostly contributed from (1×2) patches. It will have the highest normal velocity component of the desorbing CO_2 from the declining terraces. Therefore, the mean velocity would show three maxima at $\theta = 26°$ in [001] and $[00\bar{1}]$, and at $\theta = 0°$. The component in the normal direction is the contribution from (1×1) patches. In the latter case, on the other hand, the velocity should decrease smoothly with the increasing desorption angle in any direction.

B. Spatial distribution

The desorption component on (1×2) has a very sharp angular distribution of $(\cos\theta)^{18\pm2}$ dependence in the [001] direction and $(\cos\theta)^{7\pm1}$ in the $[1\bar{1}0]$ direction. This distribution is quite similar to that on Pt(110)(1×2).[4] A sharp distribution of reactive CO_2 desorption was reported on

well-polished polycrystalline iridium surfaces.[29] Such a sharp distribution indicates that CO_2 is desorbed immediately after the formation without being trapped on the surface.[5] Sharp angular distributions in reactive CO_2 desorption have been reported on several surfaces of platinum metals.[1-4,30-32] In general, molecules are produced closer to the surface than the equilibrium position of the molecular adsorption.[2] The repulsive force from the surface is exerted on the product during the formation and, therefore, the desorption is likely to be accelerated along the reaction site normal. In fact, excess translational energy has been found in the normal velocity component of desorbing CO_2 produced on Pt(111)[27] and Rh(111).[28]

The terrace on the reconstructed plane would decline at ± 35.3 deg if the surface metal atoms were located in the same position as in the bulk crystal. However, this is not the case, because the first several layers are distorted on the reconstructed surface. According to analysis with LEED,[8(b)] the declining angle is about 24 deg on the clean Ir(110)(1×2) surface. The collimation angle (the angle where the reactive CO_2 desorption flux is maximized) agrees well with this value within experimental error. This is surprising, since the fine structure around the desorption site has been thought to be obscured by the smoothing effect on the surfaces by conduction electrons. The spatial distribution was believed to be unaffected by the surface corrugation in the atomic scale.[33] The present results show that this effect has only a minor influence on reducing the collimation angle in the CO oxidation.

C. Surface quality

The surfaces of (1×1) and (1×2) used in the present experiments did not necessarily consist of pure structures. The (1×2) surface showed half-order spots that were somewhat streaked in the [001] direction. Heating at 1450 K for 10 min seems insufficient for complete transformation into the (1×2) form.[15] This suggests that the total CO_2 signal at $\theta = 0°$ on (1×2) is partly contributed from the formation on remnant (1×1) patches. The compositional ratio of 2.2 at $T_P = 1450$ K must be underestimated as the value on pure (1×2). It would be 3.2 if only the two directional desorption components of $(\cos\theta \pm 26)$[18] contribute to the signal at the bulk surface normal.

The imperfection of the surface structure was also discussed on (1×1) in the preceding section. The observed compositional ratio of about 0.8 around $T_P = 570$ K must be overestimated as the value on pure (1×1) surfaces. The surface should be examined by other methods capable for the estimation of the local surface structure, e.g., scanning tunneling microscopy (STM).[7,34]

V. SUMMARY

The spatial distribution of product desorption was studied for the oxidation of carbon monoxide on Ir(110) surfaces by using angle-resolved thermal desorption and low energy electron diffraction. The results are summarized as follows:

(1) The CO_2 formation shows two peaks at 380 and 550 K on both (1×1) and (1×2) surfaces.

(2) The spatial distribution of the CO_2 desorption at 380 K was analyzed in detail. On (1×1) surfaces, it is collimated along the surface normal, and the distribution perpendicular to the surface trough is broad, and sharper when parallel to it. The reactive desorption on a short bridge site was strongly suggested.

(3) The distribution on (1×2) shows two-directional desorption collimated along the axis at $\theta = 26°$ in both [001] and [00$\bar{1}$] directions. The reaction proceeds on declining terraces. The orientation of the reaction site is well preserved in the spatial distribution.

(4) The spatial distribution changed from the (1×1) type to the (1×2) type during the transformation of the surface structure from (1×1) into (1×2).

ACKNOWLEDGMENT

One of the authors (K. N.) is indebted to Toyota Physical and Chemical Research Institute for a scholarship.

[1] T. Matsushima, M. Hashimoto, and T. Matsui, J. Chem. Phys. **81**, 5151 (1984).
[2] T. Matsushima and H. Asada, J. Chem. Phys. **85**, 1658 (1986).
[3] T. Matsushima, J. Chem. Phys. **91**, 5722 (1989).
[4] (a) T. Matsushima and Y. Ohno, Chem. Phys. Lett. **169**, 569 (1990); (b) T. Matsushima, J. Chem. Phys. **93**, 1464 (1990).
[5] G. Comsa and R. David, Surf. Sci. Rep. **5**, 145 (1985).
[6] T. Matsushima, Y. Ohno, and K. Nagai, Surf. Sci. (in press).
[7] (a) T. Gritdch, D. Coulman, R. J. Behm, and G. Ertl, Appl. Phys. A **49**, 403 (1989); (b) Phys. Rev. Lett. **63**, 1086 (1989).
[8] (a) C. M. Chan, M. A. Van Hove, W. H. Weinberg, and E. D. Williams, Surf. Sci. **91**, 440 (1980); (b) C. M. Chan and M. A. Van Hove, *ibid.* **177**, 226 (1986).
[9] (a) T. T. Tsong and Q. -J. Gao, Surf. Sci. **182**, L257 (1987); (b) T. T. Tsong and Q. -J. Gao, J. Vac. Sci. Technol. A **5**, 761 (1987); (c) Q.-J. Gao and T. T. Tsong, Phys. Rev. B **36**, 2547 (1987).
[10] G. L. Kellogg, J. Vac. Sci. Technol. A **5**, 747 (1987).
[11] K. Müller, J. Witt, and O. Schutz, J. Vac. Sci. Technol. A **5**, 757 (1987).
[12] M. Copel, P. Fenter, and T. Gustafsson, J. Vac. Sci. Technol. A **5**, 742 (1987).
[13] S. Ferrer and H. P. Bonzel, Surf. Sci. **119**, 234 (1982).
[14] N. Freyer, M. Kiskinova, G. Pirug, and H. P. Bonzel, Appl. Phys. A **39**, 209 (1986).
[15] (a) C.-M. Chan, S. L. Cunningham, K. L. Luke, W. H. Weinberg, and S. P. Withrow, Surf. Sci. **78**, 15 (1978); (b) C.-M. Chan, K. L. Luke, M. A. Van Hove, W. H. Weinberg, and E. D. Williams, J. Vac. Sci. Technol. **16**, 642 (1979).
[16] T. Matsushima, Surf. Sci. **127**, 403 (1983).
[17] J. L. Taylor, D. E. Ibbotson, and W. H. Weinberg, J. Chem. Phys. **69**, 4298 (1978).
[18] T. Matsushima, Surf. Sci. **87**, 665 (1979).
[19] J. E. Reutt-Robey, D. J. Doren, Y. J. Chabal, and S. B. Christman, Phys. Rev. Lett. **61**, 2778 (1988).
[20] J. L. Taylor, D. E. Ibbotson, and W. H. Weinberg, Surf. Sci. **79**, 349 (1979).
[21] C.-M. Chan and W. H. Weinberg, J. Chem. Phys. **71**, 2788 (1979).
[22] C.-M. Chan, K. L. Luke, M. A. Van Hove, W. H. Weinberg, and S. P. Withrow, Surf. Sci. **78**, 386 (1978).
[23] J. F. Wendelken, Surf. Sci. **108**, 605 (1981).
[24] W. Heiland, F. Iberl, and E. Taglauer, Surf. Sci. **53**, 383 (1975).
[25] C. Backs, C. P. M. de Groot, and P. Biloen, Surf. Sci. **104**, 300 (1981).
[26] M. Nishijima, M. Jo, Y. Kuwahara, and M. Onchi, Solid State Commun. **60**, 257 (1986).
[27] C. A. Becker, J. P. Cowin, L. Wharton, and D. J. Auerbach, J. Chem. Phys. **67**, 3394 (1977).
[28] L. S. Brown and S. J. Sibener, J. Chem. Phys. **90**, 2807 (1989).

[29] T. Matsushima, J. Phys. Chem. **88**, 202 (1984).
[30] R. L. Palmer and J. N. Smith, Jr., J. Chem. Phys. **60**, 1453 (1974).
[31] C. T. Campbell, G. Ertl, H. Kuipers, and J. Segner, J. Chem. Phys. **73**, 5862 (1980).
[32] J. Segner, C. T. Campbell, G. Doyen, and G. Ertl, Surf. Sci. **138**, 505 (1984).
[33] M. Balooch, M. J. Cardillo, D. R. Miller, and R. E. Stickney, Surf. Sci. **46**, 358 (1974).
[34] G. Binnig, H. Rohler, Ch. Gerber, and E. Weibel, Surf. Sci. Lett. **131**, L379 (1983).